

Noninductive Startup of Spherical Tokamak with Reduced Trapped Electrons by Electron Bernstein Wave Heating and Current Drive on LATE

M. Uchida, H. Tanaka, H. Etou, T. Taiga, H. Shinohara, A. Nakai, R. Hirayama
Graduate School of Energy Science, Kyoto University, Kyoto 606-8502, Japan
E-mail: m-uchida@energy.kyoto-u.ac.jp

Abstract- Start up and formation of an overdense spherical tokamak by electron Bernstein waves with the microwave injection from bottom port in order to suppress trapped electrons has been investigated in the Low Aspect ratio Torus Experiment (LATE) device. The experimental results show that the development of trapped electrons outside the last closed flux surface are suppressed compared with the midplane outboard injection case, suggesting the improved coupling to current carrying passing electrons. The results also suggest that the bottom injection is advantageous for heating at the plasma core without the 2nd harmonic heating in the peripheral region.

Non-inductive start up of spherical tokamak is one of the most important issue to realize compact and economical fusion reactors. In the LATE device it was shown that electron Bernstein (EB) waves can rapidly ramp-up the plasma current as fast as ~ 260 kA/s, comparable to the lower hybrid ramp-up rate [1], and also can startup and form an extremely overdense tokamak in which the electron density reaches as high as 7 times the plasma cutoff density [2, 3]. In these previous experiments, however, trapped electrons were significantly developed in terms of energy and density outside the last closed flux surface (LCFS) and they were lost to the vacuum vessel wall via pitch angle scatterings. The total loss power amounts up to ~ 70 percent of the injected power, resulting in a severe degradation in current drive efficiency.

In order to suppress trapped electrons outside LCFS, a new bottom port launcher has been installed on the LATE device as shown in Figure 1 (f). The angle of launcher is 15 degrees from the vertical and its center line crosses the midplane at $R = 0.18$ m. The injection mode is O-mode for the mode-conversion to EB waves via O-X-B method. After the mode conversion the parallel refractive index N_{\parallel} of EB waves upshifts as the waves propagate inward when the waves are below midplane for the magnetic configuration of LATE.

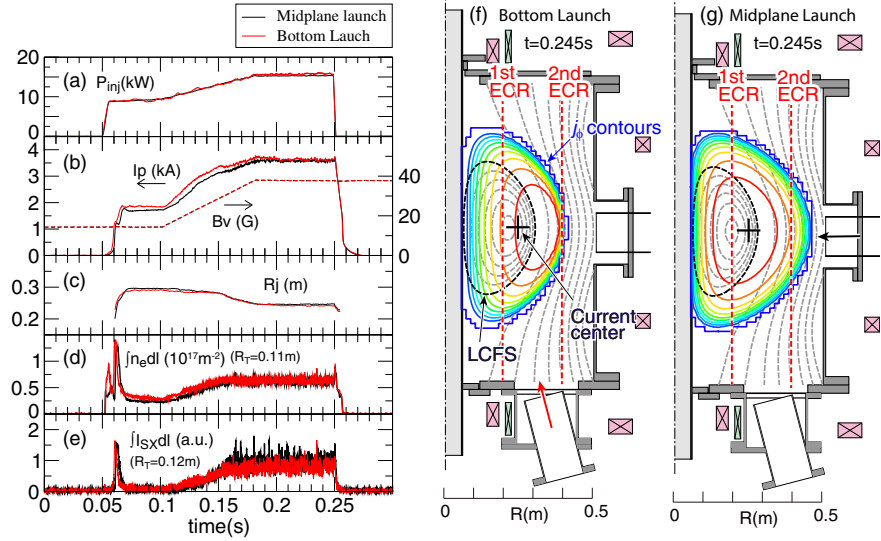


Fig.1 Typical discharges for bottom (red) and midplane (black) injection. (a)-(e) Time traces. (f), (g) Current density (color) and poloidal flux contours (gray). Contours are equally spaced. The 1st and 2nd ECR layer are shown in red dash lines.

Figure 1 shows the typical discharges comparing the bottom (red) and the midplane outboard (black) injection. When a microwave power of $P_{inj} \sim 8$ kW is injected under a weak B_v field of ~ 15 G, a plasma current is initiated and increases up to ~ 2 kA, resulting in a formation of closed flux surfaces ($t = 0.07$ s). The plasma current ramps up with ramps of the microwave power and B_v , and finally

reaches $I_p \sim 3.6$ kA, after which the plasma is maintained steady until the end of microwave pulse. The soft X-ray signal appears and increases with I_p as shown in Fig. 1(e), suggesting the current is carried by EB-wave driven fast electron tail [1].

The plasma current of bottom injection is slightly higher than that of midplane injection throughout the discharge, suggesting an improved efficiency in current generation, although the difference in I_p is not large since the equilibrium vertical field strength B_v , which is pre-programmed, constrains I_p . The traces of radial position of plasma current center, line-integrated density, and soft X-ray intensity (Figs. 1(c),(d),and(e)) are almost the same for both the injections. Figures 1(f) and 1(g) show current density and poloidal flux contours at $t = 0.245$ s estimated by the magnetic analysis [1] for bottom and midplane injection, respectively.

The current distribution for midplane injection is significantly extended to the lower field side, indicating the development of trapped electrons outside the LCFS. On the other hand, they are suppressed for the bottom injection case.

The equilibrium pressure profiles are obtained using the equation for anisotropic pressure, $\mathbf{j} \times \mathbf{B} = \nabla \cdot \mathbf{P}$ ($\mathbf{P} = p_\perp \mathbf{I} + (p_\parallel - p_\perp) \mathbf{B}\mathbf{B}/B^2$) and $\nabla \cdot \mathbf{j} = 0$, where p_\parallel and p_\perp are parallel and perpendicular pressure [1]. Figures 2(a) and (b) show sum pressure distributions of $p_\parallel + p_\perp$. Radial profiles of p_\parallel and p_\perp on midplane are shown in Figs 2(c) and (d). These indicate that the large p_\perp region outside the LCFS is suppressed and, on the other hand, p_\parallel near the magnetic axis increased in the case of bottom injection. Volume integrals of p_\perp and p_\parallel in the bottom injection case are 10 % lower and 20 % higher than those in the midplane injection, respectively. These indicate that trapped electrons outside LCFS are suppressed and efficient development of current carrying passing electrons are realized.

The electron density profiles are estimated with the 4 chord measurement of line-integrated density at tangency radii of $R_T = 0.11, 0.19, 0.27, 0.355$ m on midplane. The upper hybrid resonances are estimated to lie to higher field side of the 2nd ECR layer for both the case as shown in Figs. 2(a) and (b). Then EB waves mode converted from the incident waves propagate in their first propagation band toward the fundamental ECR layer may heat the bulk electrons as well as the fast electrons [2] for both the case. Trapped electrons extended outside the 2nd ECR layer for the midplane injection may be attributed to the 2nd ECR heating by the incident electromagnetic waves. Such trapped electrons will be lost to radial, bottom or top limiter via pitch angle scatterings. The total losses to the radial, bottom and top estimated from the temperature rise of the limiters for the midplane and bottom injection are ~ 70 % and ~ 55 % of the injected microwave energy, respectively, indicating the spatial loss to the limiters is reduced by ~ 20 % for the bottom injection. These observations indicate that the microwave absorption by trapped electrons is suppressed and efficient coupling to EB waves in the first propagation band is realized in the bottom injection case.

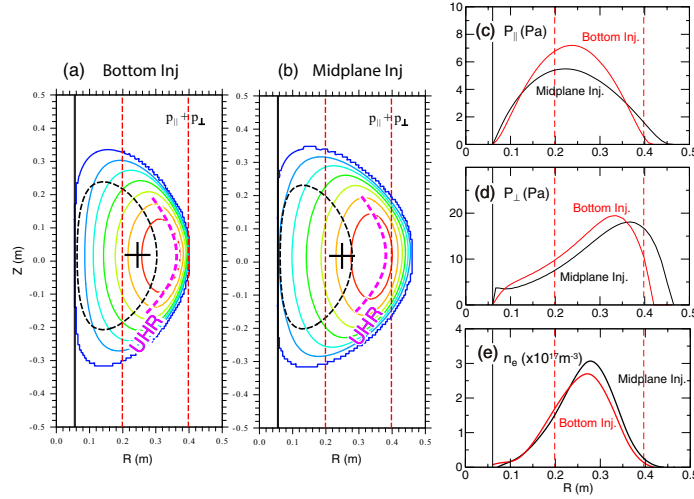


Fig.2 Profiles of various quantities of the plasma at $t = 0.245$ s in Fig.1. (a) and (b) $p_\parallel + p_\perp$ for Bottom and Midplane injection. (c) and (d) radial profiles of p_\parallel and p_\perp on midplane. (e) n_e profile on midplane.

[1] M. Uchida *et al.*, Phys. Rev. Lett. **104** 065001 (2010).

[2] M. Uchida *et al.*, Proc. 24th Int. Conf on Fusion Energy 2012 IAEA-CN-197/EX/P6-18.

[3] H. Tanaka *et al.*, Proc. 26th Int. Conf on Fusion Energy 2016 IAEA-CN/EX/P4-45.